LETTERS IN BIOMATHEMATICS
An International Journal

Intercollegiate Biomathematics Alliance

RESEARCH ARTICLE

OPEN ACCESS

An SIRS Pulse Vaccination Model with Nonlinear Incidence Rate and Time Delay

Ardak Kashkynbayev[a], Meruyert Yeleussinova[a], Shirali Kadyrov[b]

[a] Department of Mathematics, Nazarbayev University, Astana, Kazakhstan; [b] Department of Mathematics and Natural Sciences, SDU University, Kaskelen, Kazakhstan

ABSTRACT

In this paper, we investigate the effectiveness of pulse vaccination as a control strategy for a time-delayed SIRS epidemic model with varying population size. The dynamics of the infectious disease are closely tied to the basic reproduction number, denoted as R_0. Traditional epidemic models evaluate R_0 using the next generation matrix, but this approach is unsuitable for non-autonomous systems. As our study focuses on pulse vaccination strategies, our system naturally falls into the non-autonomous category. To address this, we adopt a general approach that derives R_0 in terms of spectral radii of Poincaré maps. Furthermore, we demonstrate the existence of an infectious-free periodic solution and establish its global attractiveness for $R_0 < 1$ while highlighting the persistence of the infectious disease for $R_0 > 1$. Lastly, we conduct a comprehensive sensitivity analysis for R_0 under the framework of the Holling type II functional response.

ARTICLE HISTORY
Received May 18, 2022
Accepted October 24, 2023

KEYWORDS
epidemic models, global attractiveness, spectral radius, the Poincaré map, pulse vaccination system (PVS)

1 Introduction

In the present era, improving public health has emerged as a prominent global concern, engaging individuals from all corners of the world in extensive discussions. This widespread attention is not surprising, given that people possess an inherent desire to lead healthy and prolonged lives. While the adoption of a healthy lifestyle can aid in the prevention of certain diseases, there are instances when outbreaks occur that defy conventional treatment approaches. A striking example is the recent outbreak of meningitis, which surfaced in multiple countries during the summer of 2018 (WHO, 2019). This outbreak had a significant impact on the affected population before eventually subsiding. Consequently, the field of epidemiology assumes a pivotal role in investigating the behavior of infectious diseases, mathematical modeling facilitates the prediction of epidemic thresholds. Such thresholds serve as crucial parameters in delineating the characteristics of a disease and devising effective control measures.

Epidemiological models have a rich history dating back to 1927, when Kermack and McKendrick (1927) first introduced them. Since then, numerous studies have been published, leading to advancements in formulating various models for different infectious diseases. The general form of the model is *SEIRS* model (Cooke and van den Driessche, 1996; Xu and Zhao, 2005), which consists of 4 vital epidemiological subgroups: S – susceptible, E – exposed, I – infected and R – recovered. Notably, other models such as the *SIR* model, *SI* model (Pugliese, 1990), and *SIS* model (Lou and Zhao, 2009) can be seen as specific cases of the general *SEIRS* model. These models follow a deterministic structure, wherein transmissions between classes and modifications in population size, such as births and deaths, are mathematically described using a system of differential equations that govern the time-evolution of each compartment value.

To make the model more realistic, it is necessary to take into consideration the latent period, denoted as τ, which represents a time delay. Takeuchi discusses a delayed equation for the incidence rate in relation to factor I, but not for factor S. Specifically, the incidence term can be expressed as $f\left(S(t), I(t-\tau)\right)$ (Huang et al., 2010). The current rate of new infectious people depends on the current number of susceptible people and the current number of infectious mosquitoes. For instance, with a latency period of τ, the current number of infectious mosquitoes depends on the number of infectious people τ time units ago. It is worth mentioning that in recent years, several studies have examined general incidence rate functions that satisfy mild conditions (Church and Liu, 2019; Kashkynbayev and Koptleuova, 2020; Kashkynbayev and Rihan, 2021; Korobeinikov, 2006, 2007; Korobeinikov and Maini, 2004).

CONTACT Ardak Kashkynbayev ardak.kashkynbayev@nu.edu.kz

Epidemiology has emerged due to the widespread occurrence of infectious diseases, necessitating the development of effective programs to control and prevent these infections. Various methods of vaccination have been employed to combat these diseases, including traditional approaches such as *SVIR* and *SVEIR*, where class V represents the vaccinated population (Jiang et al., 2009). In this analysis, we will focus on the impact of the pulse vaccination strategy (PVS) (Shulgin et al., 1998; Stone et al., 2000), which has proven to be an effective approach to disease control.

The primary objective of PVS (Nokes and Swinton, 1997) is to minimize the number of susceptible individuals, ensuring their direct transition to the recovered population without getting infected. This strategy involves implementing repeated vaccination actions within a population when the infection rate is on the rise, continuing until the spread of the disease has been halted. Additionally, we will consider scenarios where recovered individuals may lose their immunity over time. For instance, in the *SIR* model, individuals who have been vaccinated acquire complete immunity to the pathogen. Conversely, in the *SIRS* model, the recovered population gradually loses their immunity, making them susceptible to reinfection.

In this work, we propose a vaccination strategy aimed at preventing the occurrence of any disease, referred to as the disease-free state. Under this strategy, the susceptible population experiences a unique periodic solution known as the disease-free periodic solution (DFPS). By analyzing the dynamics of the disease-free periodic solution, we can gain insights into the effectiveness of this fixed and periodic vaccination strategy (Nokes and Swinton, 1995; Bai, 2015; Bai and Zhao, 2020).

To further investigate whether the disease dies out or persists, we analyze the basic reproduction number R_0. This analysis is conducted using the spectral radius approach, which expands upon the main results of the autonomous system (Watmough and van den Driessche, 2002). The determination of R_0 serves as a crucial factor in understanding the long-term dynamics of the disease.

In general, the concept of defining R_0 in terms of the spectral radius of the next generation matrix was initially introduced by Diekmann et al. (1990). This approach serves as an extension of the next generation matrix method.

There are numerous works on the threshold dynamics of periodic models. For instance, Xu and Zhao (2005) studied the global persistence and extinction of a periodic competitive model by analyzing the spectral radii of the Poincaré maps associated with linear periodic delay equations. The results were obtained in two values R^* and R_*, and dynamics were analyzed for two thresholds. A similar approach was followed by Yongzhen et al. (2017) to study a SIR model with two parallel infectious stages. However, Bai (2015) recently presented a paper on a single basic reproduction number for associated periodic equations with impulsive effects. The author considered a bilinear incidence rate, whereas our objective is to determine R_0 using the spectral radius approach for a generalized incidence rate. In a more recent paper, Bai and Zhao (2020) have used functional analytic methods to provide a more explicit characterization of the basic reproduction number. Church and Liu (2019) conducted a study on an SIR model with time delay, a general nonlinear incidence rate, pulse vaccination, and temporary immunity. They analyzed various types of bifurcations. On the other hand, Nie et al. (2018) proposed a state-dependent pulse vaccination strategy where the threshold value depends on the number of infected individuals. In a recent study by Davies et al. (2019), a combination of pulse vaccination and routine childhood immunization was suggested to reduce Lassa fever, which is prevalent in Sub-Saharan West Africa.

The focus of the present paper is a delayed *SIRS* model that incorporates a pulse vaccination system. The model assumes that susceptible individuals undergo a latent period after coming into contact with an infected individual. Subsequently, they become infectious and eventually recover with temporary acquired immunity.

2 Model Formulation

In this paper, we investigate the delayed *SIRS* model, taking into account a pulse vaccination system. The population is divided into three classes: the susceptible individuals (denoted by S), the infectious individuals (denoted by I), and the recovered individuals (denoted by R). The model can be described as follows:

$$\begin{cases} \left.\begin{aligned} \frac{dS}{dt} &= \Lambda - \mu S(t) - f(S(t), I(t-\tau)) + \alpha R(t), \\ \frac{dI}{dt} &= f(S(t), I(t-\tau)) - (\mu + d + \delta) I(t), \\ \frac{dR}{dt} &= \delta I(t) - \mu R(t) - \alpha R(t), \end{aligned}\right\} t \neq k\omega, k \in \mathbb{N} \\ \left.\begin{aligned} \Delta S(t) &= -\theta S(t), \\ \Delta I(t) &= 0, \\ \Delta R(t) &= \theta S(t), \end{aligned}\right\} t = k\omega, k \in \mathbb{N} \end{cases} \tag{1}$$

where $\Delta x(t) = x(t+) - x(t-)$, and the coefficients Λ, μ, α, and δ are positive constants. The recruitment rate of the population is denoted by Λ, the natural death rate is denoted by μ, the rate of losing immunity is denoted by α, and the recovery rate is

denoted by δ. Additionally, the infectious compartment has an extra disease-related death rate denoted as d. The parameter τ is the average length of the latent period, and ω is the period between successive vaccinations. We let $\theta \in (0,1)$ denote the fraction of susceptible individuals who are successfully vaccinated at times $t = k\omega$. We let $\mathbb{C}(X, Y)$ and $\mathbb{PC}(X, Y)$ denote the space of continuous and piecewise continuous functions from a topological space X to a topological space Y, respectively. Further, let us define $\mathbb{C}_\omega(\mathbb{R})$ to be the Banach space of all continuous and ω - periodic functions from $\mathbb{R}$ to $\mathbb{R}$ equipped with the norm $||u|| = \max_i |u_i|$. For a function $x \in \mathbb{C}([-\tau, \nu], \mathbb{R}^n)$, $\nu > 0$, we define $x_t \in \mathbb{C}([-\tau, 0], \mathbb{R}^n)$ by $x_t(\zeta) = x(t + \zeta)$, for all $\zeta \in [-\tau, 0]$, $t \in [0, \nu]$.

We consider the system (1) with the following initial conditions

$$S(\xi) = \psi_1(\xi),\ I(\xi) = \psi_2(\xi),\ R(\xi) = \psi_3(\xi), \tag{2}$$

where $\psi_1, \psi_3 \in \mathbb{PC}([-\tau, 0], \mathbb{R})$, $\psi_2 \in \mathbb{C}([-\tau, 0], \mathbb{R})$ and satisfy $\psi_1(0) > 0$, $\psi_2(0) \geq 0$, and $\psi_3(0) \geq 0$. It worth mentioning that Theorem 1.2.3 and Theorem 1.2.4 from Fu et al. (2005) yield that the system (1) supplemented with the initial condition (2) has a unique solution for $t \geq 0$.

Further, we will assume that the following assumptions hold for the function f in system (1):

(H1) $f(S, 0) = f(0, I) = 0$;

(H2) $f(S, I)$ is always positive, continuous, differentiable and monotonically increasing i.e., $\dfrac{\partial f(S,I)}{\partial S} > 0$ and $\dfrac{\partial f(S,I)}{\partial I} > 0$ for all $S > 0$ and $I \geq 0$;

(H3) $f(S, I)$ is concave with respect to I.

The assumptions **(H1)**–**(H3)** keep the model biologically feasible. The assumption **(H1)** means that there can be no transmission if there is no infected or susceptible individual left. In **(H2)**, we assume that the transmission is positive for positive susceptible and nonnegative infected populations. Further, the transmission increases as S and I increase. Finally, in **(H3)**, we assume that the transmission rate exhibits a saturation effect with respect to the number of infected individuals (I). This means that as I continues to increase, the rate of transmission gradually levels off or slows down. See papers by Huang et al. (2010), Zhao (2017), and Korobeinikov (2007) with a transition function satisfying similar assumptions.

Lemma 2.1 (Gao et al., 2006). *Let's consider the following impulsive system*

$$\begin{cases} \dfrac{dz}{dt} = a - bz(t), & t \neq k\omega \\ \Delta z(t) = -\theta z, & t = k\omega, \end{cases}$$

where $a > 0, b > 0, 0 < \theta < 1$. Then there exists a unique positive periodic solution of the above system

$$\tilde{z}(t) = \frac{a}{b} + \left(z^* - \frac{a}{b}\right)e^{-b(t-k\omega)},\ k\omega < t \leq (k+1)\omega,$$

which is globally asymptotically stable, where $z^* = \dfrac{a}{b}\dfrac{(1-\theta)(1-e^{-b\omega})}{1-(1-\theta)e^{-b\omega}}$.

3 The Basic Reproduction Number

The total population size is determined by $N(t) = S(t) + I(t) + R(t)$. Summing all equations in the system (1) yields

$$\frac{dN}{dt} = \Lambda - \mu N(t) - dI(t).$$

Thus, we can deduce that $\Lambda - (\mu + d)N(t) \leq \dfrac{dN}{dt} \leq \Lambda - \mu N(t)$. From the last inequality, the following conclusion can be drawn:

$$\frac{\Lambda}{\mu + d} \leq \liminf_{t\to\infty} N(t) \leq \limsup_{t\to\infty} N(t) \leq \frac{\Lambda}{\mu}.$$

Hence, it is sufficient to consider the system (1) in a biologically feasible closed set denoted as

$$\Omega = \left\{(S, I, R) \in \mathbb{R}_+ \middle| \, 0 \le S + I + R \le \frac{\Lambda}{\mu}\right\}.$$

It can be easily verified that the set Ω is positively invariant with respect to (1), meaning that any solution of (1) starting in Ω remains within this closed set for $t \ge 0$.

Next, we demonstrate the existence of a disease-free periodic solution, where the population is considered to be free of infections, i.e., $I(t) = 0$ for all $t \ge 0$. In the limiting system, we have the following relationship:

$$R(t) = \frac{\Lambda}{\mu} - S(t)$$

since $\limsup_{t\to\infty} N(t) = \frac{\Lambda}{\mu}$. Therefore, the system (1) in the limiting case can be simplified to:

$$\begin{cases} \dfrac{dS}{dt} = \left(\dfrac{\Lambda}{\mu} - S(t)\right)(\alpha + \mu), & t \ne k\omega \\ \Delta S(t) = -\theta S, & t = k\omega. \end{cases} \tag{3}$$

By applying Lemma 2.1, we can deduce that the system (3) possesses a unique positive ω-periodic solution, which can be expressed using the following formula:

$$\tilde{S}(t) = \frac{\Lambda}{\mu} + \left(S^* - \frac{\Lambda}{\mu}\right) e^{-(\mu+\alpha)(t-k\omega)}, \; k\omega < t \le (k+1)\omega,$$

where $S^* = \dfrac{\Lambda}{\mu} \dfrac{(1-\theta)(1-e^{-(\mu+\alpha)\omega})}{(1-(1-\theta)e^{-(\mu+\alpha)\omega})}$. It is worth noting that the stability of $\tilde{S}(t)$ is guaranteed to be globally asymptotic, as stated in Lemma 1. Therefore, we can conclude that the group of recovered individuals exhibits oscillations with the same period ω. As a result, the system (1) always possesses a disease-free periodic solution given by:

$$E_0 = \left(\tilde{S}(t), 0, \frac{\Lambda}{\mu} - \tilde{S}(t)\right).$$

In order to analyze the dynamics of the epidemic model (1), it is crucial to determine the threshold value known as the basic reproduction number, denoted by R_0. Due to the discontinuous nature of the system (1), the traditional approach using the next generation matrix technique (Watmough and van den Driessche, 2002) cannot be employed to obtain R_0. Due to the discontinuous nature of the system (1), the traditional approach using the next generation matrix technique (Watmough and van den Driessche, 2002) cannot be employed to obtain R_0. However, in our case, we can utilize a more general approach based on the spectral radius (Bai and Zhao, 2020). Alternatively, due to the specific structure of our model, we can adopt a simpler approach proposed by Zhao (2017). By linearizing the system (1) around the disease-free periodic solution E_0, we derive the following linear periodic functional differential equation governing the behavior of the infected population.

$$\frac{dI}{dt} = \frac{\partial f(\tilde{S}(t), 0)}{\partial I} I(t-\tau) - (\mu + d + \delta) I(t). \tag{4}$$

Consider the linear ordinary differential equation:

$$\frac{dI}{dt} = -(\mu + d + \delta) I(t). \tag{5}$$

Let $\Phi(t, s)$ denote the principal fundamental matrix associated with this equation, where $\Phi(s, s) = 1$ for all $s \in \mathbb{R}$. It is straightforward to observe that $\Phi(t, s) = e^{-(t-s)(\mu+d+\delta)}$, for all $t \ge s$. Let us further define $g(t) := \dfrac{\partial f(\tilde{S}(t), 0)}{\partial I}$ and an operator Π as $\Pi(t)\varphi = g(t)\varphi(-\tau)$ for any $\varphi \in \mathbb{C}([-\tau, 0], \mathbb{R})$. One can show that $\Pi(t)\varphi = \int_{-\tau}^{0} d_\eta[\sigma(t, \eta)]\varphi(\eta)$, $\forall t \in \mathbb{R}$, $\varphi \in \mathbb{C}([-\tau, 0], \mathbb{R})$, where $\sigma(t, \eta)$ is the normalized function satisfying

$$\sigma(t, \eta) = \begin{cases} -g(t), & \eta \le -\tau, \\ 0, & \text{otherwise.} \end{cases}$$

By virtue of condition **(H2)**, it can be concluded that both Π and $\sigma(t, \eta)$ fulfill all the requirements outlined by Zhao (2017, see Section 2). Namely, $\sigma(t, \eta)$ is a measurable function in $(t, \eta) \in \mathbb{R} \times \mathbb{R}$ and a left-continuous function in η on $(-\tau, 0)$.

Furthermore, it can be demonstrated that the variation of $\sigma(t,\cdot)$ on $[-\tau,0]$ is bounded by $g(t)$. On the other hand, since $\Pi(t)$ is $\omega-$periodic, we have $\sup_{t\in\mathbb{R}}\|\Pi(t)\| = \sup_{t\in[0,\omega]}\|\Pi(t)\| \leq \sup_{t\in[0,\omega]} g(t)$. Thus, we define two linear operators on $\mathbb{C}_\omega$ as follows.

$$\mathcal{M}y(t) = \Pi(t)\left(\int_0^\infty \Phi(t+\cdot, t-s+\cdot)y(t-s+\cdot)\,ds\right),\ \forall t\in\mathbb{R},\ y\in\mathbb{C}_\omega,$$

and

$$\mathcal{N}y(t) = \int_0^\infty \Phi(t,t-s)\Pi(t-s)y(t-s+\cdot)\,ds,\ \forall t\in\mathbb{R},\ y\in\mathbb{C}_\omega.$$

Note that the spectral radii of the operators $\mathcal{M}$ and $\mathcal{N}$ are equal. This can be observed by considering two bounded linear operators, U and V, on $\mathbb{C}_\omega$ defined as follows:

$$Uy(t) = \int_0^\infty \Phi(t,t-s)y(t-s)\,ds \text{ and } Vy(t) = \Pi(t)y_t,\ y\in\mathbb{C}_\omega.$$

It follows that $\mathcal{M} = V\circ U$ and $\mathcal{N} = U\circ V$. Hence, the spectral radii of $\mathcal{M}$ and $\mathcal{N}$ are equal. As a result, following the procedures outlined by Zhao (2017), we can conclude that the basic reproduction number, denoted as R_0, is defined as the spectral radius of either the operator $\mathcal{M}$ or the operator $\mathcal{N}$, i.e., $R_0 := r(\mathcal{M}) = r(\mathcal{N})$. Let us continue with $R_0 = r(\mathcal{M})$. We observe that

$$\begin{aligned}
\mathcal{M}y(t) &= \Pi(t)\left(\int_0^\infty \Phi(t+\cdot,t-s+\cdot)y(t-s+\cdot)\,ds\right)\\
&= g(t)\int_0^\infty \Phi(t-\tau,t-s-\tau)y(t-s-\tau)\,ds\\
&= g(t)\int_\tau^\infty \Phi(t-\tau,t-s)y(t-s)\,ds\\
&= g(t)\int_\tau^\infty e^{-(\mu+d+\delta)(s-\tau)}y(t-s)ds.
\end{aligned}$$

Thus, R_0 satisfies the following eigenvalue problem.

$$R_0y(t) = g(t)\int_\tau^\infty e^{-(\mu+d+\delta)(s-\tau)}y(t-s)ds. \tag{6}$$

Differentiating the last equation yields

$$\begin{aligned}
R_0y'(t) &= g(t)\int_\tau^\infty e^{-(\mu+d+\delta)(s-\tau)}y'(t-s)ds + g'(t)\int_\tau^\infty e^{-(\mu+d+\delta)(s-\tau)}y(t-s)ds\\
&= -g(t)e^{-(\mu+d+\delta)(s-\tau)}y(t-s)\Big|_\tau^\infty - g(t)(\mu+d+\delta)\int_\tau^\infty e^{-(\mu+d+\delta)(s-\tau)}y(t-s)ds\\
&\quad + \frac{g'(t)}{g(t)}g(t)\int_\tau^\infty e^{-(\mu+d+\delta)(s-\tau)}y(t-s)ds\\
&= g(t)y(t-\tau) - (\mu+d+\delta)R_0y(t) + \frac{g'(t)}{g(t)}R_0y(t).
\end{aligned}$$

The last equations leads to

$$\frac{y'(t)}{y(t)} = \frac{g'(t)}{g(t)} + \frac{g(t)}{R_0}\frac{y(t-\tau)}{y(t)} - (\mu+d+\delta).$$

Observe that $y(\omega) = y(0)$ and $g(\omega) = g(0)$. Integrating the last expression from 0 to ω yields

$$R_0 = \frac{1}{\omega(\mu+d+\gamma)}\int_0^\omega g(t)\frac{y(t-\tau)}{y(t)}dt = \frac{1}{\omega(\mu+d+\gamma)}\int_0^\omega \frac{\partial f(\tilde{S}(t),0)}{\partial I}\frac{y(t-\tau)}{y(t)}dt. \tag{7}$$

In the absence of time-delay, $\tau = 0$, the last formula yields

$$R_0 = \frac{1}{\omega(\mu+d+\gamma)}\int_0^\omega \frac{\partial f(\tilde{S}(t),0)}{\partial I}dt.$$

Note that the operator $\mathcal{M}$ can be rewritten as

$$\mathcal{M}y(t) = \int_0^\infty K(t,s)y(t-s)ds, \tag{8}$$

where the kernel function $K(t,s)$ is given by

$$K(t,s) = \begin{cases} g(t-s+\tau)e^{-(\mu+d+\delta)(s-\tau)}, & \text{if } s \geq \tau, \\ 0, & \text{if } s < \tau. \end{cases}$$

4 Global Attractiveness

Let us define for any $\phi \in \mathbb{C}([-\tau,0],\mathbb{R})$, an operator $P(t)$ such that $P(t)\phi = u_t(\phi)$ is the unique solution of the system (4). Then, it follows that $P := P(\omega)$ is the Poincaré map of the system (4). In what follows, we will utilize Theorem 2.1 and Theorem 3.1 from Zhao (2017) in the proof of our results. Therefore, we present these theorems below for reference:

Lemma 4.1 (Zhao, 2017, see Theorem 2.1). *Let $r(P)$ be a spectral radius of P. Then $sign(R_0 - 1) = sign(r(P) - 1)$, i.e., R_0 and $r(P)$ have the same threshold value.*

Lemma 4.2 (Zhao, 2017, see Theorem 3.1). *Let $\mu = \dfrac{\ln r(P)}{\omega}$, then there exists a positive $\omega-$periodic function $v(t)$ such that $e^{\mu t}v(t)$ is a positive solution of the system (4).*

Theorem 4.1. *The disease-free periodic solution of system (1) $\left(\tilde{S}(t), 0, \dfrac{\Lambda}{\mu} - \tilde{S}(t)\right)$ be globally attractive if $R_0 < 1$, then the disease-free periodic solution E_0 is globally attractive for system (1) in $PC([-\tau,0],\mathbb{R}^3_+)$.*

Proof. Note that from the system (1) it follows that

$$\frac{dS}{dt} \leq (\alpha+\mu)\left(\frac{\Lambda}{\mu} - S(t)\right).$$

Thus, we consider the following comparison equation for the system (1):

$$\begin{cases} \dfrac{d\tilde{S}}{dt}(t) = (\alpha+\mu)\left(\dfrac{\Lambda}{\mu} - \tilde{S}(t)\right), & t \neq k\omega, \\ \Delta\tilde{S}(t) = -\theta\tilde{S}(t), & t = k\omega. \end{cases}$$

By utilizing Lemma 2.1, we can establish the existence of a globally asymptotically stable positive periodic solution denoted by $\tilde{S}^*(t)$ for the aforementioned system. Applying the comparison theorem for impulsive differential equations (Lakshmikantham et al., 1989), we can conclude the existence of a natural number $n_1 > 0$ satisfying the inequality:

$$S(t) < \tilde{S}(t) < \tilde{S}(t) + \varepsilon, \quad k\omega < t \leq (k+1)\omega,\ k > n_1.$$

As a result, under the condition **(H2)**, there exists another natural number $n_2 > n_1$ such that the following condition holds for $t \geq t_1 = n_2\omega + \tau$.

$$\frac{dI}{dt} \leq \frac{df(\tilde{S}(t)+\varepsilon, 0)}{dI} I(t-\tau) - (\mu+d+\delta)I(t).$$

Next, we consider the following perturbed system.

$$\frac{d\bar{I}}{dt} = \frac{df(\tilde{S}(t)+\varepsilon, 0)}{dI} \bar{I}(t-\tau) - (\mu+d+\delta)\bar{I}(t). \tag{9}$$

Let P_ε denote the Poincaré map of the equation (9). According to Lemma 4.1, $R_0 < 1$ if and only if $r(P) < 1$. Moreover, the inequality $\lim_{\varepsilon\to 0} r(P_\varepsilon) = r(P) < 1$ holds since the operator r is compact and continuous in the operator norm with respect to ε (Kato, 1995). Thus, we fix a sufficiently small number $\varepsilon > 0$ such that $r(P_\varepsilon) < 1$. By Lemma 4.2, there exists a positive ω-periodic function $v_\varepsilon(t)$ such that $e^{\mu_\varepsilon t}v_\varepsilon(t)$ is a positive solution of (9), where $\mu_\varepsilon = \dfrac{\ln(r(P_\varepsilon))}{\omega} < 0$. Furthermore, applying the

comparison theorem for impulsive differential equations (Lakshmikantham et al., 1989), we can find a suitably large $H > 0$ such that

$$I(t) \leq He^{\mu_\varepsilon t} v_\varepsilon(t), \text{ for all } t \geq t_1.$$

Thus, from the inequality above we conclude that

$$\lim_{t\to\infty} I(t) = 0.$$

On the other hand, we have shown that $N(t)$ satisfies $\dfrac{\Lambda}{\mu+d} \leq \liminf_{t\to\infty} N(t) \leq \limsup_{t\to\infty} N(t) \leq \dfrac{\Lambda}{\mu}$. Thus, for $\varepsilon_1 > 0$ there exists a natural number n_3 with $n_3\omega > t_1$ such that

$$I(t) < \varepsilon_1 \quad \text{and} \quad \frac{\Lambda}{\mu+d} - \varepsilon_1 < N(t) < \frac{\Lambda}{\mu} + \varepsilon_1, \quad \text{for} \quad t > n_3\omega. \tag{10}$$

Using the inequalities in (10), the condition **(H2)**, and the fact that $S(t) \leq N(t)$, we obtain the following inequality

$$\begin{aligned}
\frac{dS}{dt} &= \Lambda - f(S(t), I(t-\tau)) - \mu S(t) + \alpha(N(t) - S(t) - I(t)) \\
&\geq \Lambda - f\left(\frac{\Lambda}{\mu} + \varepsilon_1, \varepsilon_1\right) - \mu S(t) + \alpha\left(\frac{\Lambda}{\mu+d} - \varepsilon_1 - S(t) - \varepsilon_1\right) \\
&= \left(\Lambda + \frac{\alpha\Lambda}{\mu+d} - f\left(\frac{\Lambda}{\mu} + \varepsilon_1, \varepsilon_1\right) - 2\alpha\varepsilon_1\right) - (\alpha+\mu)S(t).
\end{aligned}$$

We consider the system

$$\begin{cases}
\dfrac{d\tilde{S}_{\varepsilon_1}}{dt} = \left(\Lambda + \frac{\alpha\Lambda}{\mu+d} - f\left(\frac{\Lambda}{\mu} + \varepsilon_1, \varepsilon_1\right) - 2\alpha\varepsilon_1\right) - (\alpha+\mu)\tilde{S}_{\varepsilon_1}(t), & t \neq k\omega \\
\Delta\tilde{S}_{\varepsilon_1}(t) = -\theta\tilde{S}_{\varepsilon_1}, & t = k\omega.
\end{cases} \tag{11}$$

Lemma 2.1 implies that the system (11) has globally stable $\omega-$periodic solution $\tilde{S}_{\varepsilon_1}$. By employing the comparison principle for impulsive systems once again we conclude that there exists a natural number n_4 such that

$$\tilde{S}_{\varepsilon_1} \leq S(t) < \tilde{S}(t) + \varepsilon_1, \; k\omega < t < (k+1)\omega, \; k > n_4.$$

As ε_1 is chosen arbitrarily small and $\lim_{\varepsilon_1\to 0} \tilde{S}_{\varepsilon_1}(t) = \tilde{S}(t)$, from the above inequalities it follows that

$$\lim_{t\to\infty} S(t) = \tilde{S}(t).$$

We conclude the proof by realizing that $\lim_{t\to\infty}\left(R(t) - \left(\dfrac{\Lambda}{\mu} - \tilde{S}(t)\right)\right) = 0$. □

Theorem 4.2. *If $R_0 > 1$, then there is a $p > 0$ such that every positive solution $u(t,\phi) = (S(t), I(t), R(t))$ of (1) satisfies $\liminf_{t\to\infty} I(t) \geq p$, for large enough value of t and any $\phi \in PC([-\tau, 0], \mathbb{R}^3_+)$, where $\phi_2(0) > 0$.*

Proof. If $R_0 > 1$ Lemma 4.1 yields $r(P) > 1$. Let P_γ be the Poincaré map of the perturbed equation below

$$\frac{dI}{dt} = \left(\frac{\partial f(\tilde{S}(t) - \gamma, 0)}{\partial I}\right) I(t-\tau) - (\mu + d + \delta) I(t). \tag{12}$$

Let us fix a sufficiently small number $\gamma > 0$, such that $r(P_\gamma) > 1$ and $\gamma < \inf_{t\geq 0} \tilde{S}(t)$ as $\lim_{\gamma\to 0} r(P_\gamma) = r(P) > 1$.

By Lemma 4.2 we obtain a positive solution $e^{\mu_\gamma t} v_\gamma(t)$ of (12), where $v_\gamma(t)$ is a positive $\omega-$periodic function and $\mu_\gamma = \dfrac{\ln r(P_\gamma)}{\omega} > 0$. Let us consider the following system

$$\begin{cases}
\dfrac{d\bar{S}}{dt}(t) = \left(\Lambda + \dfrac{\alpha A}{\mu} - f\left(\dfrac{\Lambda}{\mu} + \varepsilon, \varepsilon\right) - 2\alpha\varepsilon\right) - (\alpha+\mu)S(t), & t \neq k\omega, \\
\Delta\bar{S}(t) = -\theta\bar{S}(t), & t = k\omega.
\end{cases}$$

Lemma 2.1 indicates that this system possesses a globally asymptotically stable positive periodic solution $\tilde{S}\varepsilon(t)$, which can be expressed as $\lim \varepsilon \to 0(\tilde{S}\varepsilon(t) - \tilde{S}(t)) = 0$. Consequently, we select a sufficiently small $\varepsilon > 0$ to ensure that

$$\tilde{S}_\varepsilon(t) > \tilde{S}(t) - \frac{\gamma}{2}, \text{ for all } t \geq 0. \tag{13}$$

Next, we choose a small number $\eta > 0$ such that $\eta < \min\left\{\frac{\mu}{\Lambda}\varepsilon, \varepsilon\right\}$ and assume that $I(t) < \eta$ for all $t \geq t_0$ with any $t_0 > 0$. In this scenario, it follows that $I(t) < \eta < \varepsilon$, and

$$\frac{dN}{dt} = \Lambda - \mu N(t) - dI(t) > \Lambda - \mu N(t) - d\varepsilon.$$

The above inequality implies that there exits $t_1 > t_0$ such that

$$N(t) \geq \frac{\Lambda - d\varepsilon}{\mu} - \varepsilon, \text{ for all } t \geq t_1.$$

Thus, for any $t \geq t_1, t \neq k\omega$, we have

$$\frac{dS}{dt} = \Lambda - \mu S(t) - f(S(t), I(t-\tau)) + \alpha\left(N(t) - S(t) - I(t)\right) > \left(\Lambda + \frac{\alpha\Lambda}{\mu} - f\left(\frac{\Lambda}{\mu} + \varepsilon, \varepsilon\right) - 2\alpha\varepsilon\right) - (\alpha + \mu)S(t).$$

By applying the standard comparison theorem and combining it with the inequality (13), we can conclude the existence of $t_2 > t_1$ such that the following inequality holds for all $t \geq t_2$:

$$S(t) \geq \tilde{S}(t) > \tilde{S}_\varepsilon(t) - \frac{\gamma}{2} > \tilde{S}(t) - \gamma. \tag{14}$$

Furthermore, since the function f is monotone with respect to S and concave with respect to I, we can deduce that for $t \geq t_3 = t_2 + \tau$, where τ is a specific value,

$$\begin{aligned}\frac{dI}{dt} &= f(S(t), I(t-\tau)) - (\mu + d + \delta)I(t)\\ &\geq f(\tilde{S}(t) - \gamma, I(t-\tau)) - (\mu + d + \delta)I(t)\\ &\geq \left(\frac{\partial f(\tilde{S} - \gamma, 0)}{\partial I}\right) I(t-\tau) - (\mu + d + \delta)I(t).\end{aligned}$$

Let us choose a positive number K_2 such that

$$I(t) \geq K_2 e^{\mu_\gamma t} v_\gamma(t) \quad \text{and} \quad K_2 e^{\mu_\gamma t} v_\gamma(t) < \eta, \text{ for } t \in [t_2, t_3].$$

Then by the comparison theorem (Smith, 1995) there exists $t_4 > t_3$ such that $\eta \leq I(t) < \varepsilon$ for $t \in [t_3, t_4]$. This is a contradiction to our assumption that $I(t) < \eta$. Thus, it follows that either

(i) $I(t) \geq \eta$ for all sufficiently large t.

or

(ii) $I(t)$ oscillates about η for all sufficiently large t.

It is clear that if (i) is true, then Theorem 4.2 is proved. Thus, we need to show Theorem 4.2 holds true in the case (ii). Let us define $p = \min\left\{\frac{\eta}{2}, \eta e^{-(\mu+d+\delta)\tau}\right\}$ and take T_1 and T_2 such that

$$I(T_1) = I(T_2) = \eta, \; I(t) < \eta, \text{ for } t \in (T_1, T_2),$$

where T_1 is considered to be sufficiently large to satisfy

$$S(t) > \tilde{S}(t) - \gamma, \text{ for } t \in [T_1, T_2]. \tag{15}$$

Note that $I(t)$ is uniformly continuous for any $t \geq 0$ since the infectious compartment $I'(t)$ of our model (1) is bounded for all $t \geq 0$. Hence, there exits $t^* \in (0, \tau)$ such that $I(t) \geq \frac{\eta}{2}$ for $[T_1, T_1 + t^*]$. In what follows, we consider all possible cases regarding t^*.

(a) If $T_2 - T_1 \le t^*$, then $I(t) > \dfrac{\eta}{2}$, $\forall\, t \in [T_1, T_2]$.

(b) If $t^* < T_2 - T_1 \le \tau$, then $I(t) \ge e^{-(\mu+d+\delta)\tau} = \eta e^{-(\mu+d+\delta)\tau}$ for $t \in [T_1, T_2]$ since $I'(t) \ge -(\mu+d+\delta)I(t)$ and $I(T_1) = \eta$.

(c) If $T_2 - T_1 > \tau$, we obtain $I(t) \ge e^{-(\mu+d+\delta)\tau} = \eta e^{-(\mu+d+\delta)\tau}$ for $t \in [T_1, T_1 + \tau]$. We claim the same inequality holds for $t \in [T_1 + \tau, T_2]$.

Suppose it does not hold. Then, there exits $t_1^* > 0$ such that $I(t) \ge \eta e^{-(\mu+d+\delta)\tau}$ for all $t \in [T_1, T_1 + \tau + t_1^*]$, $I(T_1 + \tau + t_1^*) = \eta e^{-(\mu+d+\delta)\tau}$, and $I(t) < \eta e^{-(\mu+d+\delta)\tau}$, for $0 < t - (T_1 + \tau + t_1^*) \ll 1$. Thus, by means of (15) we have

$$\frac{dI}{dt} > \left(\frac{\partial f(\tilde{S}(t) - \gamma, 0)}{\partial I}\right) I(t-\tau) - (\mu + d + \delta) I(t), \text{ for } 0 < t - (T_1 + \tau + t_1^*) \ll 1.$$

Let us choose a number $K_3 > 0$ such that

$$I(t) \ge K_3 e^{\mu_\gamma t} v_\gamma(t), \text{ for}, t \in [T_1 + t_1^*, T_1 + \tau + t_1^*] \text{ and } K_3 e^{\mu_\gamma (T_1 + t_1^*)} \min_{\forall t \in [0,\tau]} v_\gamma(t) \ge e^{-(\mu+d+\delta)\tau}.$$

Applying the comparison theorem yields

$$I(t) \ge e^{-(\mu+d+\delta)\tau}, \text{ for } 0 < t - (T_1 + \tau + t_1^*) \ll 1$$

which contradicts the assumption. Thus, we get $I(t) \ge p$, for all $t \in [T_1, T_2]$. Since this interval was chosen arbitrarily, we conclude that for large enough t the following inequality holds

$$I(t) \ge p.$$

This finalizes the proof. □

5 Numerical Approximations and Sensitivity Analysis

While it is that the basic reproduction number R_0 depends on pulse vaccination parameters θ and ω, the explicit relationship is not apparent from formula (7). In this section, we will explore a numerical approximation of R_0 and simulate its dependency on θ and ω. To accomplish this, we will employ the discretization approach proposed by Bacaër and Guernaoui (2006). To this end, we substitute $x = t - s$ in (6) and using ω-periodicity of y to obtain

$$\begin{aligned} R_0 y(t) &= g(t) \int_{-\infty}^{t-\tau} e^{-(\mu+d+\delta)(t-\tau-x)} y(x)\, dx \\ &= g(t) \left(\int_0^{t-\tau} e^{-(\mu+d+\delta)(t-\tau-x)} y(x)\, dx + \sum_{n=0}^{\infty} \int_{-\omega(n+1)}^{-\omega n} e^{-(\mu+d+\delta)(t-\tau-x)} y(x)\, dx \right) \\ &= g(t) \left(\int_0^{t-\tau} e^{-(\mu+d+\delta)(t-\tau-x)} y(x)\, dx + \sum_{n=0}^{\infty} \int_0^{\omega} e^{-(\mu+d+\delta)(t-\tau+(n+1)\omega-x)} y(x)\, dx \right). \end{aligned}$$

Interchanging the summation with the integral and noticing that

$$\sum_{n=0}^{\infty} e^{-(\mu+d+\delta)(t-\tau+(n+1)\omega-x)} = \frac{e^{-(\mu+d+\delta)(t-\tau+\omega-x)}}{1 - e^{-(\mu+d+\delta)\omega}}$$

we arrive at

$$R_0 y(t) = g(t) \left(\int_0^{t-\tau} e^{-(\mu+d+\delta)(t-\tau-x)} y(x)\, dx + \int_0^{\omega} \frac{e^{-(\mu+d+\delta)(t-\tau+\omega-x)}}{1 - e^{-(\mu+d+\delta)\omega}} y(x)\, dx \right). \tag{16}$$

Now that we have the integrals over finite intervals, we can approximate the variable y using vectors by employing discretization. For the sake of simplicity, we may assume that the incubation period τ is less that the vaccination periods ω. For any natural number N we define $t_i = i\omega/N$ for $i = 0, 1, 2, \ldots, N$. These points partition the interval $[0, \omega]$ into N equal sub-intervals so that the periodic and continuous function y can be approximated by N-dimensional column vector $Y = (Y_0, Y_1, \ldots, Y_{N-1})^T$

for sufficiently large N, where we set $Y_i := y(t_i)$. In other words, for any t_i, where $i = 0, 1, \ldots, N-1$, we can approximate the second integral in Equation (16) as a Riemann sum:

$$\int_0^{\omega} \frac{e^{-(\mu+d+\delta)(t_i-\tau+\omega-x)}}{1-e^{-(\mu+d+\delta)\omega}} y(x)\,dx = \lim_{N\to\infty} \frac{\omega}{N} \sum_{j=0}^{N-1} \frac{e^{-(\mu+d+\delta)(t_i-\tau+\omega-t_j)}}{1-e^{-(\mu+d+\delta)\omega}} Y_j.$$

On the other hand, the first integral depends on whether $t-\tau$ is positive or negative. Let k be such that $t_k \le \tau < t_{k+1}$ so that $t_i - t_{k+1} < t_i - \tau \le t_i - t_k$. Then, if $i > k$ we have $t_i - t_k = t_{i-k}$ so that

$$\int_0^{t_i-\tau} e^{-(\mu+d+\delta)(t-\tau-x)} y(x)\,dx = \lim_{N\to\infty} \frac{\omega}{N} \sum_{j=0}^{i-k} e^{-(\mu+d+\delta)(t_i-\tau-t_j)} Y_j.$$

If $i \le k$, then

$$\int_0^{t_i-\tau} e^{-(\mu+d+\delta)(t_i-\tau-x)} y(x)\,dx = -\int_{\omega+t_i-\tau}^{\omega} e^{-(\mu+d+\delta)(t_i-\tau+\omega-x)} y(x)\,dx = \lim_{N\to\infty} -\frac{\omega}{N} \sum_{j=N+i-k}^{N-1} e^{-(\mu+d+\delta)(t_i-\tau+\omega-t_j)} Y_j.$$

Putting all of this together, we observe that for sufficiently large N, the spectral radius ρ_0 which satisfies the eigenvalue problem

$$\rho_0 Y = AY$$

provides a reliable approximation for R_0, where A is an $N \times N$ matrix with entries

$$A_{ij} = \frac{g(t_i)\omega e^{-(\mu+d+\delta)(t_i-\tau+\omega-t_j)}}{N(1-e^{-(\mu+d+\delta)\omega})} + \frac{g(t_i)\omega}{N} \cdot \begin{cases} e^{-(\mu+d+\delta)(t_i-\tau-t_j)} & \text{if } i > k \text{ and } j \le i-k, \\ 0 & \text{if i > k and } j > i-k, \\ -e^{-(\mu+d+\delta)(t_i-\tau+\omega-t_j)} & \text{if } i \le k \text{ if } j \ge N+i-k, \\ 0 & \text{if } i \le k \text{ if } j < N+i-k. \end{cases} \tag{17}$$

We consider $f(S,I) = \beta SI/(N+\eta S)$ where β represents the transmission rate and η represents the saturation rate. In our simulation, we specifically focused on capturing the dynamics of COVID-19 in Kazakhstan, and to ensure consistency, we set the parameter values according to Table 1. It is important to note that we implemented the simulation using the Python 3 programming language. We have included the appropriate references in Table 1 for parameters that have been previously documented in the literature. While our parameters may exhibit slight variations compared to the referenced sources, it is important to acknowledge the presence of conflicting findings in the field of parameter estimation, as numerous research studies have reported disparate results. However, for parameters that are not explicitly mentioned in previous studies, we have ensured that they fall within a legitimate interval. The legitimate interval refers to a range of values that are considered plausible and reasonable for the given context. While we cannot provide specific references for these parameters, their values have been carefully selected based on expert knowledge, empirical data, or theoretical considerations. The choice of parameter values within the legitimate interval is crucial to ensure the validity and accuracy of the numerical simulation. Finally, it should be noted that the accuracy of parameter values does not play a crucial role in sensitivity analysis. Using these parameter values, we can now estimate the basic reproduction number, R_0, through the numerical approximation ρ_0 described earlier.

We know that with $N \to \infty$ the spectral radius ρ_0 of an $N \times N$ matrix equals R_0. The Figure 1 presents the results of approximation for values of $N \le 1000$. It is evident that for N greater than 500, we obtain a reliable estimation of R_0, which is approximately 0.83.

To simulate the disease dynamics we fix initial values to be $S(0) = N(0), I(0) = 20000$, and $R(0) = 200000$. We first examine the dynamics in the absence of vaccination, which implies $\beta = 0$. In this scenario, the basic reproduction number is calculated to be $R_0 = 2.19$, and the simulation results are presented in Figure 2. It can be observed that the system tends towards an endemic equilibrium.

If we keep $\theta = 0.4$ as in Table 1 then the system approaches to disease free periodic solution E_0 described in Section 3. This is in accordance with Theorem 4.1, given that $R_0 = 0.83 < 1$.

On the other hand, if we reduce the vaccination rate to $\beta = 0.1$, then the system becomes unstable with $R_0 = 1.63$, as depicted in Figure 4. In this case, the disease continues to persist, which aligns with Theorem 4.2.

For sensitivity analysis, as outlined by Li (2018), we present the *elasticity* of R_0 with respect to a parameter λ, denoted as $\varepsilon_{R_0}^{\lambda}$. It is computed using the formula:

$$\varepsilon_{R_0}^{\lambda} = \frac{\partial R_0}{\partial \lambda} \frac{\lambda}{R_0}.$$

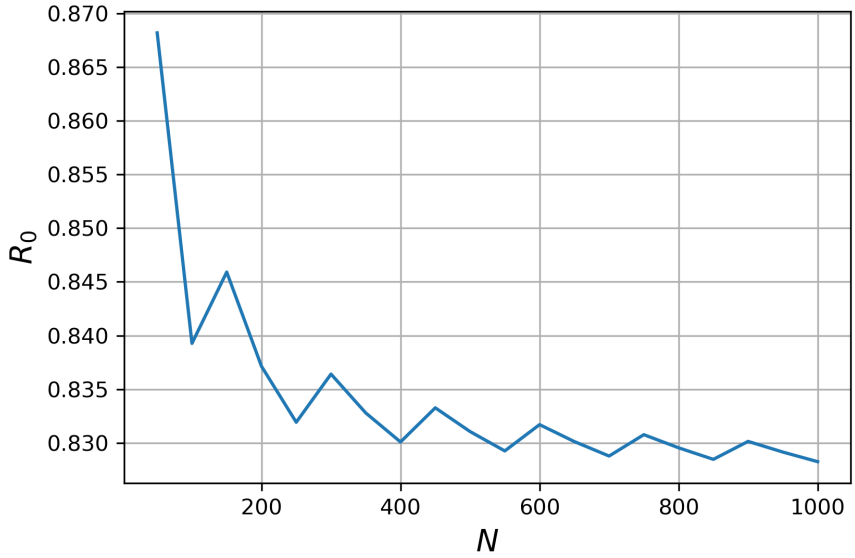

Figure 1: Numerical estimation of R_0.

Table 1: Baseline parameter values and local sensitivity analysis.

Parameter	Variable	Base Value	Reference	Elasticity
Total population	$N(0)$	18000000	BNS, 2022	−1.00
Recruitment rate of population	Λ	1000 days^{-1}	BNS, 2022	1.00
Natural death rate	μ	0.00004 days^{-1}	BNS, 2022	−1.00
Transmission rate	β	0.015 days^{-1}		1.00
Latent period	τ	7 days	Balram et al., 2021	0.83
Rate of loosing immunity	α	0.01 days^{-1}	Nick et al., 2022	0.63
Recovery rate	δ	0.07 days^{-1}	Elsawah et al., 2021	−0.84
Disease-related death rate	d	0.015 days^{-1}	Bakasis et al., 2021	−0.16
Vaccination period	ω	30 days		−0.04
Vaccination rate	θ	0.4 days^{-1}		−0.78
Saturation rate	η	0.001 days^{-1}		−0.0005

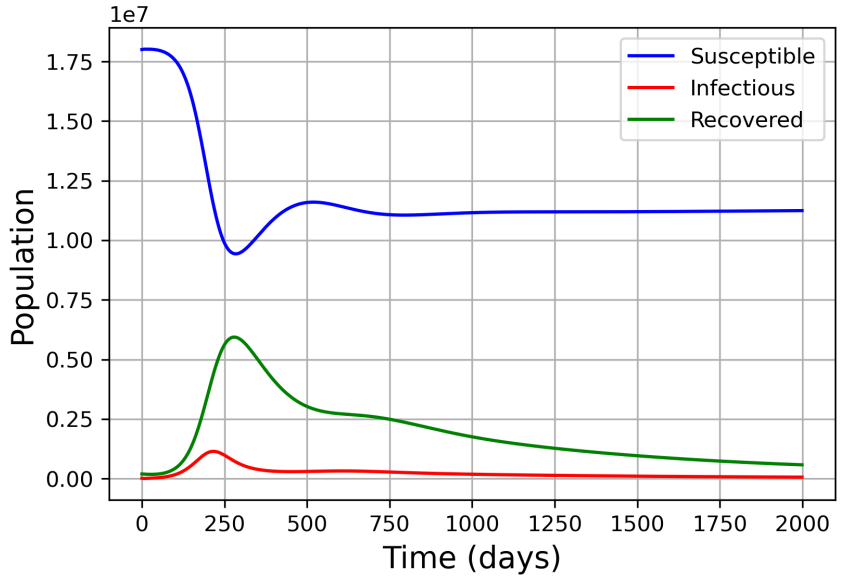

Figure 2: Disease dynamics without vaccination, $R_0 = 2.19$.

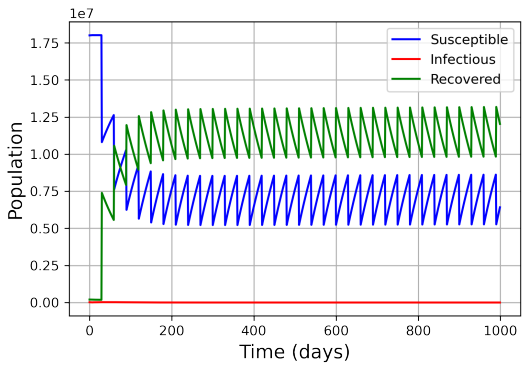

(a) Dynamics with vaccination

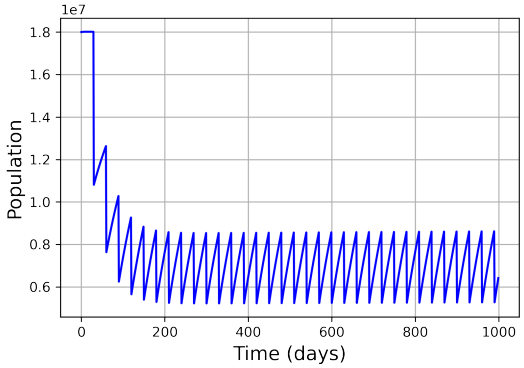

(b) Susceptible

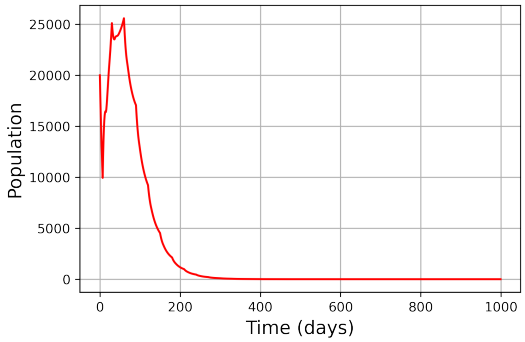

(c) Infectious

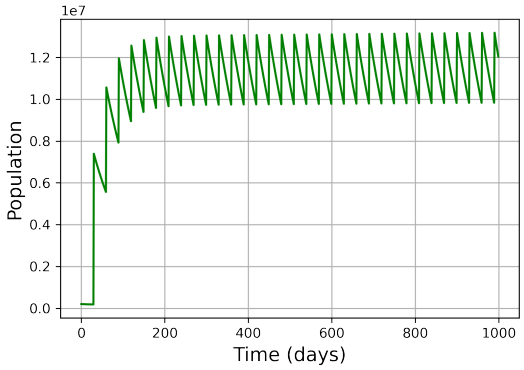

(d) Recovered

Figure 3: Disease dynamics with vaccination rate $\theta = 0.4$ and $R_0 = 0.83$.

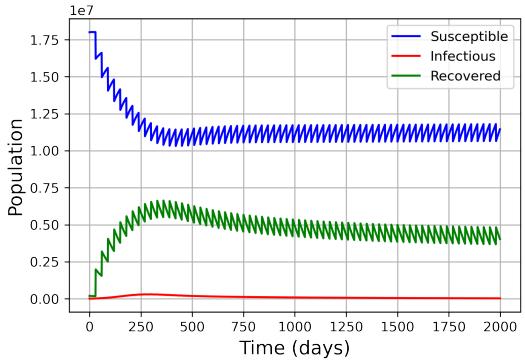

(a) Dynamics with vaccination

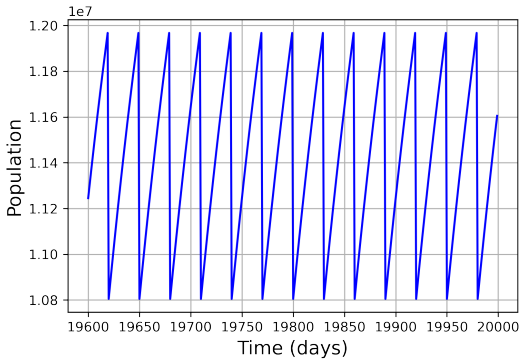

(b) Susceptible

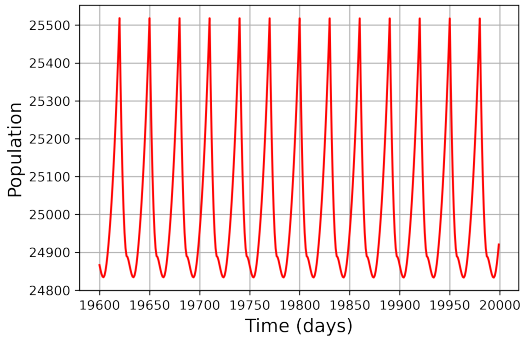

(c) Infectious

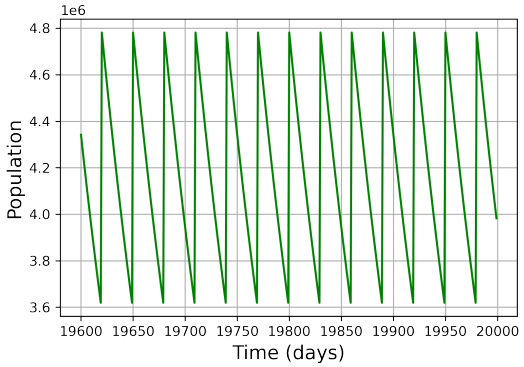

(d) Recovered

Figure 4: Disease dynamics with vaccination rate $\theta = 0.1$ and $R_0 = 1.63$.

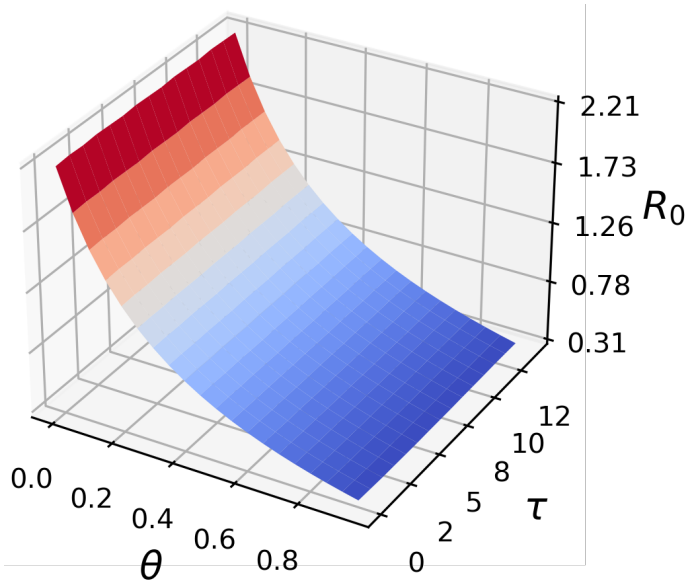

Figure 5: Sensitivity of R_0 to τ and θ.

To this end, we approximate partial derivatives numerically employing the approximation $\frac{\partial R_0}{\partial \lambda} \approx \frac{\Delta R_0}{\Delta \lambda}$ with a small increment $\Delta\lambda = 10^{-10}\lambda$. The results of analysis are presented in the last column of Table 1. For example, $\varepsilon^{\theta}_{R_0} = -0.78$ means that 1% change in the vaccination rate $\theta = 0.4$ leads to -0.78% change in the reproduction number $R_0 = 0.83$. On the other hand, $\varepsilon^{\beta}_{R_0} = 1$ suggests that 1% increase transmission rate β increases R_0 by 1% which is higher than $\varepsilon^{\theta}_{R_0} = -0.78$. We note that the transmission rate can be regulated through measures such as social distancing (e.g., lockdown measures) and awareness campaigns. However, it is important to consider that strict lockdown measures may have more significant economic impacts compared to vaccination strategies.

Although elasticity analysis provides valuable insights into local sensitivity, it may not capture the overall global picture. In order to obtain a comprehensive understanding, we conducted a global sensitivity analysis of R_0 with respect to both the latent period τ and the vaccination rate θ, as depicted in Figure 5.

Our findings reveal that variations in the latent period τ have a negligible impact on R_0. This suggests that changes in the duration between infection and the onset of infectiousness have little effect on the reproduction number.

We also report the sensitivity of R_0 to vaccination period ω, see Figure 6

6 Discussion and Conclusion

In this article, we study non-autonomous epidemic model SIRS with pulse vaccination and nonlinear incidence. Under mild conditions, we prove the global stability of disease-free periodic solution when the basic reproduction number is less than 1, cf. Theorem 4.1. Moreover, when $R_0 > 1$, we show in Theorem 4.2 that the disease free periodic solution is unstable, and the disease persists. Our second numerical simulation, see Figure 4, suggests that, in fact when $R_0 > 1$, the endemic periodic solution should be globally stable. This could be an interesting research question to explore in the future.

In our study, we express the basic reproduction number R_0 as the spectral radius of an operator and derive an exact formula when the latent period τ is 0. Additionally, we obtain a numerical approximation for R_0. Furthermore, we conduct a sensitivity analysis of R_0 with respect to various epidemiological parameters. To this end, we estimate the elasticity for each parameter, as presented in Table 1.

One unexpected observation is that the elasticity of R_0 with respect to the vaccination period ω is negative. This implies that an increase in the pulse vaccination periods might lead to a decrease in R_0. The estimated elasticity of R_0 with respect to the vaccination period ω is calculated to be -0.04, which is equivalent to -4%. Despite the magnitude, this value is considered insignificant. However, based on the insights provided by the global dynamics depicted in Figure 6, we expect the elasticity to be positive. It is important to note that due to the lack of an explicit formula for R_0, we relied on a numerical approach for approximation. Additionally, since it is not possible to compute partial derivatives of R0 with respect to ω directly, we resorted to numerical approximation once again. We believe that the observed negative elasticity with respect to ω could potentially be attributed to numerical approximation errors.

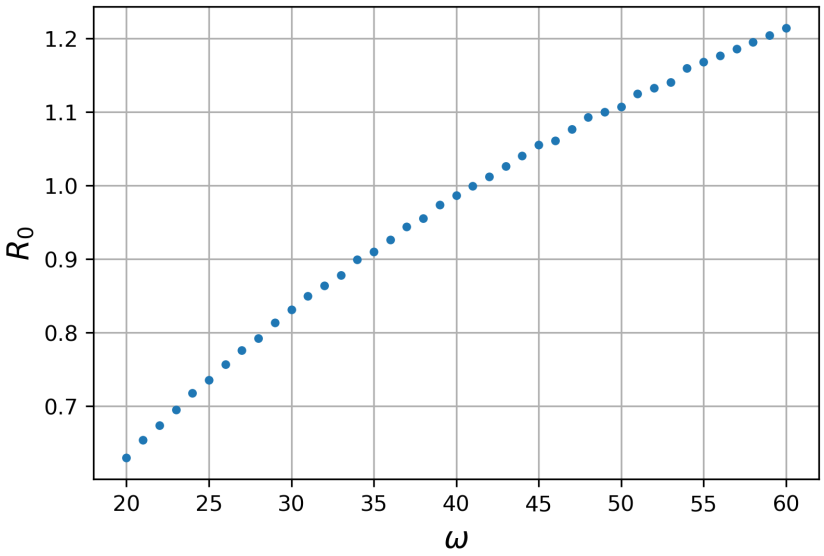

Figure 6: Global sensitivity of R_0 to vaccination period ω.

Acknowledgments

The authors would like to acknowledge that this research is funded by the Science Committee of the Ministry of Science and Higher Education of the Republic of Kazakhstan Grant No. AP13068282 "Synchronization and anti-synchronization analysis of discrete-time neural networks with delays" and in part by the Nazarbayev University, Kazakhstan under Collaborative Research Program Grant No. 11022021CRP1509.

References

Bacaër, N. and S. Guernaoui (2006). The epidemic threshold of vector-borne diseases with seasonality. *Journal of Mathematical Biology 53*(3), 421–436. 141

Bai, Z. (2015). Threshold dynamics of a periodic SIR model with delay in an infected compartment. *Math. Biosci. Eng. 12*, 555. 134

Bai, Z. and X. Zhao (2020). Basic reproduction ratios for periodic and time-delayed compartmental models with impulses. *Journal of Mathematical Biology 80*, 1095–1117. 134, 136

Bakasis, A. D., C. P. Mavragani, K. A. Boki, A. G. Tzioufas, P. G. Vlachoyiannopoulos, I. E. Stergiou, F. N. Skopouli, and H. M. Moutsopoulos (2021). COVID-19 infection among autoimmune rheumatic disease patients: data from an observational study and literature review. *Journal of Autoimmunity 123*, 102687. 143

Balram, R., A. Shukla, and L. K. Dwivedi (2021). Incubation period for COVID-19: a systematic review and meta-analysis. *Journal of Public Health*, 1–8. 143

Bureau of National Statistics (2022). Official Website of the Bureau of National Statistics. `https://stat.gov.kz/`. [Accessed: January 5, 2022] 143

Church, K. E. M. and X. Liu (2019). Analysis of a SIR model with pulse vaccination and temporary immunity: Stability, bifurcation and a cylindrical attractor. *Nonlinear Analysis: Real World Applications 50*, 240–266. 133, 134

Cooke, K. L. and P. van den Driessche (1996). Analysis of an SEIRS epidemic model with two delays. *Journal of Mathematical Biology 35*, 240-260. 133

Davies, J., K. Lokuge, and K. Glass (2019). Routine and pulse vaccination for Lassa virus could reduce high levels of endemic disease: A mathematical modelling study. *Vaccine 37*(26), 3451–3456. 134

Diekmann, O., J. A. P. Heesterbeek, J. A. J. Metz (1990). On the definition and the computation of the basic reproduction ratio R_0 in models for infectious diseases in heterogeneous populations. *Journal of Mathematical Biology 28*, 365–382. 134

Elsawah, H. K., M. A. Elsokary, M. S. Abdallah, and A. H. ElShafie (2021). Efficacy and safety of remdesivir in hospitalized Covid-19 patients: systematic review and meta-analysis including network meta-analysis. *Reviews in medical virology 31*(4), e2187. 143

Fu, X., B. Yan, and Y. Liu (2005). *Introduction of Impulsive Differential Systems*. Beijing: Science Press. 135

Gao, S., L. Chen, and Z. Teng (2006). Impulsive Vaccination of an SEIRS Model with Time Delay and Varying Total Population Size. *Bull. Math. Biol. 69*, 731–745. 135

Huang, G., Y. Takeuchi, W. Ma, and D. Wei (2010). Global stability for delay SIR and SEIR epidemic models with nonlinear incidence rate. *Bulletin of Mathematical Biology 72*, 1192–1207. 133, 135

Hui, J. and L. Chen (2004). Impulsive vaccination of SIR epidemic models with nonlinear incidence rates. *Discrete and Continuous Dynamical Systems - Series B 4*(3), 595–605.

Jiang, Y., H. Wei, X. Song, L. Mei, G.i Su, S. Qiu (2009). Global attractivity and permanence of a delayed SVEIR epidemic model with pulse vaccination and saturation incidence. *Applied Mathematics and Computation 213*, 312–321. 134

Kashkynbayev, A. and D. Koptleuova (2020). Global dynamics of tick-borne diseases. *Mathematical Biosciences and Engineering 17*(4), 4064–4079. 133

Kashkynbayev, A. and F. Rihan (2021). Dynamics of fractional-order epidemic models with general nonlinear incidence rate and time-delay. *Mathematics 9*(15), 1829. 133

Kato, T. (1995). *Perturbation Theory for Linear Operators*. Berlin: Springer-Verlag. 138

Kermack, W. O. and A. G. McKendrick (1927). A contribution to the mathematical theory of epidemics. *Proceedings of the Royal Society of London Series A 115*(772), 700–721. 133

Korobeinikov, A. (2006). Lyapunov functions and global stability for SIR and SIRS epidemiological models with non-linear transmission. *Bull. Math. Biol. 68*, 615–626. 133

Korobeinikov, A. (2007). Global Properties of Infectious Disease Models with Nonlinear Incidence. *Bull. Math. Biol. 69*, 1871–1886. 133, 135

Korobeinikov, A. and P. K. Maini (2004). A Lyapunov function and global properties for SIR and SEIR epidemiological models with nonlinear incidence. *Math. Biosci. Eng. 1*, 57–60. 133

Kuang, Y. (1993). *Delay Differential Equations with Applications in Population Dynamics*. San Diego: Academic Press Inc.

Lakshmikantham, V., D. D. Bainov, and P. S. Simeonov (1989). *Theory of Impulsive Differential Equations*. Singapore: World Scientific. 138, 139

Li, M. Y. (2018). *An introduction to mathematical modeling of infectious diseases*. Springer. 142

Lou, Y. and X. Q. Zhao (2009). Threshold dynamics in a time-delayed periodic SIS epidemic model. *Discret. Contin. Dyn. Syst. Ser. B 12*, 169–186. 133

Nick, A., J. Stowe, F. Kirsebom, S. Toffa, R. Sachdeva, C. Gower, M. Ramsay, and J. L. Bernal (2022). Effectiveness of COVID-19 booster vaccines against COVID-19-related symptoms, hospitalization and death in England. *Nature medicine 28*(4), 831–837. 143

Nie, L. F., J. Y. Shen, and C. X. Yang (2018). Dynamic behavior analysis of SIVS epidemic models with state-dependent pulse vaccination. *Nonlinear Analysis: Hybrid Systems 27*, 258–270. 134

Nokes, D. J. and J. Swinton (1995). The control of childhood viral infections by pulse vaccination. *IMA Journal of Mathematics Applied in Medicine and Biology 12*, 29–53. 134

Nokes, D. J. and J. Swinton (1997). Vaccination in pulses: A strategy for global eradication of measles and polio. *Trends in Microbiology 5*(1), 14–19. 134

Pugliese, A. (1990). *Population models for diseases with no recovery, J. Math. Biol. 28*, 65–82 133

Shulgin, B., L. Stone, and Z. Agur (1998). Pulse vaccination strategy in the SIR epidemic mode. *Bulletin of Mathematical Biology 60*, 1123–1148. 134

Smith, H. (1995). *Monotone Dynamical Systems: An Introduction to the Theory of Competitive and Cooperative Systems, Volume 41 of Mathematical Surveys and Monographs.* American Mathematical Society. 140

Stone, L., B. Shulgin, and Z. Agur (2000). Theoretical examination of the pulse vaccination policy in the SIR epidemic models. *Math. Comput. Model. 31*, 207. 134

Watmough, P. J. and P. van den Driessche (2002). Reproduction numbers and sub-threshold endemic equilibria for compartmental models of disease transmission. *Math. Biosci. 180*, 29–48. 134, 136

World Health Organization (2019). https://www.who.int/mediacentre/infographic/meningitis/meningitis-2018-2019.pdf?ua=1 133

Xu, D. and X. Q. Zhao (2005). Dynamics in a periodic competitive model with stage structure. *J.Math.Anal.Appl. 311*, 417–438. 133, 134

Yongzhen, P., L. Shuping, G. Shujing, and Z. Min (2017). Pulse vaccination of an epidemic model with two parallel infectious stages and time delays. *Mathematics and Computers in Simulation 142*, 51–61. 134

Zhang, J., J. Jia, and X. Song (2014). Analysis of an SEIR epidemic model with saturated incidence and saturated treatment function. *The Scientific World Journal.*

Zhao, S., L. Chen, and X. Song (2008). Impulsive vaccination of SEIR epidemic model with time delay and nonlinear incidence rate. *Mathematics and Computers in Simulation 79*, 500–510.

Zhao, X. Q. (2003). *Dynamical Systems in Population Biology*. New York: Springer.

Zhao, X. Q. (2017). Basic reproduction ratios for periodic compartmental models with time delay. *J. Dyn. Differ. Equ. 29*, 67–82. 135, 136, 137, 138